Inorg. Chem. **2003**, *42*, 2908–2918

Electron Donor–Acceptor Dyads Based on Ruthenium(II) Bipyridine and Terpyridine Complexes Bound to Naphthalenediimide

Olof Johansson,[†] Magnus Borgström,[‡] Reiner Lomoth,[‡] Magnus Palmblad,[§] Jonas Bergquist,[§] Leif Hammarström,*[,‡] Licheng Sun,[†] and Björn Åkermark*[,†]

Department of Organic Chemistry, Arrhenius Laboratory, Stockholm University, 106 91 Stockholm, Sweden, Department of Physical Chemistry, Uppsala University, P.O. Box 579, 751 23 Uppsala, Sweden, and Department of Analytical Chemistry, Uppsala University, P.O. Box 599, 751 24 Uppsala, Sweden

Received June 24, 2002

Two series of photosensitizer–electron acceptor complexes have been synthesized and fully characterized: ruthenium(II) tris(bipyridine) {$[Ru^{II}(bpy)_2(bpy\text{-}X\text{-}NDI)]$, where X = $-CH_2-$, tolylene, or phenylene, bpy is 2,2′-bipyridine, and NDI is naphthalenediimide} and ruthenium(II) bis(terpyridine) {$[Ru^{II}(Y\text{-}tpy)(tpy\text{-}X\text{-}NDI)]$, where Y = H or tolyl and X = tolylene or phenylene, and tpy = 2,2′:6′,2″-terpyridine}. The complexes have been studied by cyclic and differential pulse voltammetry and by steady state and time-resolved absorption and emission techniques. Rates for forward and backward electron transfer have been investigated, following photoexcitation of the ruthenium(II) polypyridine moiety. The terpyridine complexes were only marginally affected by the linked diimide unit, and no electron transfer was observed. In the bipyridine complexes we achieved efficient charge separation. For the complexes containing a phenyl link between the ruthenium(II) and diimide moieties, our results suggest a biphasic forward electron-transfer reaction, in which 20% of the charge-separated state was formed via population of the naphthalenediimide triplet state.

Introduction

The interest in mimicking the photoinduced charge separation occurring in natural photosynthesis has guided many research groups in the design of synthetic analogues. This has led to the development of multicomponent systems containing donor and/or acceptor units attached to the photosensitizer, creating long-lived charge-separated states in which solar energy is stored as chemical energy.[1−3] Photoactive transition metal complexes, especially the polypyridines of ruthenium(II) and osmium(II), have played a major role due to their favorable photophysical behavior.[4−8] Both ruthenium(II) bis(terpyridine) ($[Ru(tpy)_2]^{2+}$) and ruthenium(II) tris(bipyridine) ($[Ru(bpy)_3]^{2+}$) have been widely used as sensitizers, where the $[Ru(tpy)_2]^{2+}$ unit offers the advantage of a C_2 axis running through the 4′-position of the terpyridine ligand.[8] For the $[Ru(bpy)_3]^{2+}$ analogue, the arrangement of one donor and one acceptor component in the 4-position on two bipyridines unavoidably leads to isomers.[9] This has important consequences, since only one possible isomer, the trans isomer, has the optimum arrangement of the donor/acceptor components in terms of separation distance. The advantage of the $[Ru(bpy)_3]^{2+}$ unit is a longer excited-state lifetime as compared to the $[Ru(tpy)_2]^{2+}$, due to low-lying dd states of the latter.[8] A number of different acceptors have been linked to the ruthenium(II) polypyridine sensitizer. Viologens are the most widely used,[10−20] but also quinones[21−25] and naphthalenediimides[26,27] have been shown

[†] Stockholm University.
[‡] Department of Physical Chemistry, Uppsala University.
[§] Department of Analytical Chemistry, Uppsala University.

(1) Gust, D.; Moore, T. A.; Moore, A. L. Covalently Linked Systems Containing Porphyrin Units. In *Electron Transfer in Chemistry*; Balzani, V., Ed.; WILEY−VCH: Weinheim, 2001; pp 272−336.
(2) Scandola, F.; Chiorboli, C.; Indelli, M. T.; Rampi, M. A. Covalently Linked Systems Containing Metal Complexes. In *Electron Transfer in Chemistry*; Balzani, V., Ed.; WILEY−VCH: Weinheim, 2001; pp 337−408.
(3) Wasielewski, M. R. *Chem. Rev.* **1992**, *92*, 435−461.
(4) Balzani, V.; Juris, A.; Venturi, M.; Campagna, S.; Serroni, S. *Chem. Rev.* **1996**, *96*, 759−833.
(5) Juris, A.; Balzani, V.; Barigelletti, F.; Campagna, S.; Belser, P.; von Zelewsky, A. *Coord. Chem. Rev.* **1988**, *84*, 85−277.
(6) Kalyanasundaram, K. *Photochemistry of Polypyridine and Porphyrin Complexes*; Academic Press Limited: London, 1992.
(7) Meyer, T. J. *Acc. Chem. Res.* **1989**, *22*, 163−170.
(8) Sauvage, J.-P.; Collin, J.-P.; Chambron, J.-C.; Guillerez, S.; Coudret, C.; Balzani, V.; Barigelletti, F.; De Cola, L.; Flamigni, L. *Chem. Rev.* **1994**, *94*, 993−1019.
(9) Keene, F. R. *Coord. Chem. Rev.* **1997**, *166*, 121−159.

10.1021/ic020420k CCC: $25.00
Published on Web 04/02/2003

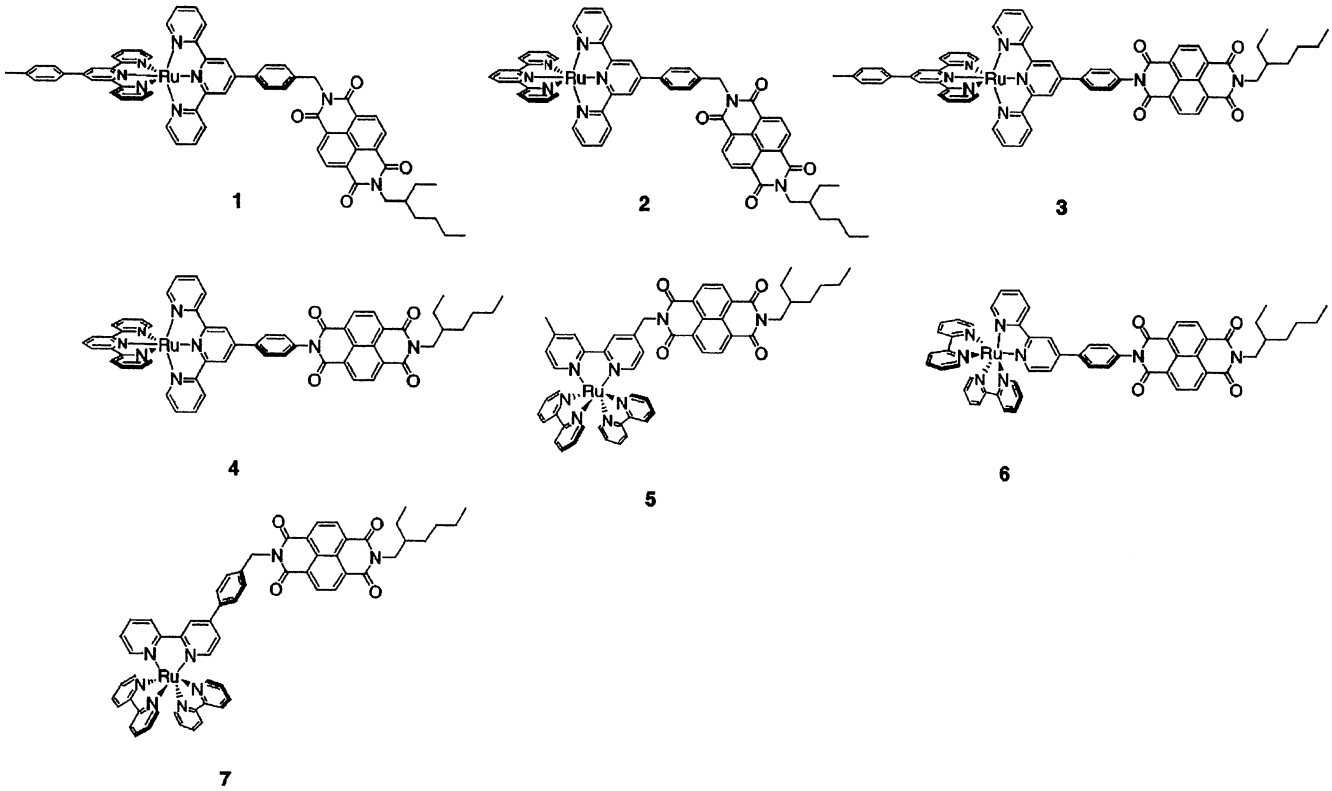

Figure 1. Structures of ruthenium(II) polypyridine complexes with linked naphthalenediimide **1**−**7**. (Isolated as PF_6^- salts.)

to work as acceptors. All of these offer different possibilities in terms of synthesis, redox and spectroscopic properties, and stability. The diimide acceptors can be expected to be more robust than both the quinones and the viologens, and the radical anions often have characteristic absorptions, which allow facile detection.

After light absorption and charge separation, the chemical potential stored in various donor−acceptor assemblies is usually lost by charge recombination. In triads and tetrads, etc., the increased distance between the charges usually increases the lifetime of the charge-separated state, but at the cost of reducing the stored energy. Ideally, a catalyst that could accumulate reductive equivalents and convert these to stable energy-rich compounds should be incorporated early in the electron-transfer chain.

In photosensitizer−acceptor (P−A) dyads, the acceptor chosen should have sufficiently low redox potential to ensure a high energy content of the charge-separated state and should ideally have a characteristic absorption in the reduced state to allow unambiguous identification of the charge-separated state. The optimal P−A system should form the P^+-A^- state with high quantum yield and sufficiently long lifetime to allow secondary reactions. Further, the P−A system should be easy to modify chemically in order to link additional redox units. In this study, we have prepared a number of P−A dyads based on both $[Ru(bpy)_3]^{2+}$ and $[Ru(tpy)_2]^{2+}$ as photosensitizers and naphthalenediimide (NDI) as acceptor, in an attempt to optimize the primary charge separation (Figure 1). The naphthalenediimide acceptor has all the previously mentioned properties. There are a few previous reports where naphthalenediimide has been linked to $[Ru(bpy)_3]^{2+}$-type sensitizers.[26,27] In these complexes, the link between donor and acceptor has been fairly flexible, leaving room for a range of different conformations. The

(10) Collin, J.-P.; Guillerez, S.; Sauvage, J.-P.; Barigelletti, F.; De Cola, L.; Flamigni, L.; Balzani, V. *Inorg. Chem.* **1991**, *30*, 4230−4238.
(11) Cooley, L. F.; Headford, C. E. L.; Elliott, C. M.; Kelley, D. F. *J. Am. Chem. Soc.* **1988**, *110*, 6673−6682.
(12) Kelly, L. A.; Rodgers, M. A. J. *J. Phys. Chem.* **1995**, *99*, 13132−13140.
(13) Lomoth, R.; Häupl, T.; Johansson, O.; Hammarström, L. *Chem. Eur. J.* **2002**, *8*, 102−110.
(14) Hu, Y.-Z.; Tsukiji, S.; Shinkai, S.; Oishi, S.; Hamachi, I. *J. Am. Chem. Soc.* **2000**, *122*, 241−253.
(15) Larson, S. L.; Cooley, L. F.; Elliott, C. M.; Kelley, D. F. *J. Am. Chem. Soc.* **1992**, *114*, 9504−9509.
(16) Larson, S. L.; Elliott, C. M.; Kelley, D. F. *J. Phys. Chem.* **1995**, *99*, 6530−6539.
(17) Maxwell, K. A.; Sykora, M.; DeSimone, J. M.; Meyer, T. J. *Inorg. Chem.* **2000**, *39*, 71−75.
(18) Mecklenburg, S. L.; Peek, B. M.; Erickson, B. W.; Meyer, T. J. *J. Am. Chem. Soc.* **1991**, *113*, 8540−8542.
(19) Treadway, J. A.; Chen, P.; Rutherford, T. J.; Keene, F. R.; Meyer, T. J. *J. Phys. Chem. A* **1997**, *101*, 6824−6826.
(20) Yonemoto, E. H.; Saupe, G. B.; Schmehl, R. H.; Hubig, S. M.; Riley, R. L.; Iverson, B. L.; Mallouk, T. E. *J. Am. Chem. Soc.* **1994**, *116*, 4786−4795.
(21) Arounaguiri, S.; Maiya, B. G. *Inorg. Chem.* **1999**, *38*, 842−843.
(22) Beer, P. D.; Timoshenko, V.; Maestri, M.; Passaniti, P.; Balzani, V. *Chem. Commun.* **1999**, 1755−1756.
(23) Berthon, R. A.; Colbran, S. B.; Moran, G. B. *Inorg. Chim. Acta* **1993**, *204*, 3−7.
(24) Goulle, V.; Harriman, A.; Lehn, J.-M. *J. Chem. Soc., Chem. Commun.* **1993**, 1034−1036.
(25) Opperman, K. A.; Mecklenburg, S. L.; Meyer, T. J. *Inorg. Chem.* **1994**, *33*, 5295−5301.
(26) Dixon, D. W.; Thornton, N. B.; Steullet, V.; Netzel, T. *Inorg. Chem.* **1999**, *38*, 5526−5534.
(27) Hossain, D.; Haga, M.; Monjushiro, H.; Gholamkhass, B.; Nozaki, K.; Ohno, T. *Chem. Lett.* **1997**, 573−574.

lifetimes of the charge-separated states were also relatively short, on the order of 300 ps.[27] This may be compared with some complexes with acceptors of the viologen type (25−300 ps)[11−13] and quinones (1 ns to a few nanoseconds).[24,25] To ensure low conformational mobility and to strive for a slower charge recombination reaction, we have synthesized a number of structurally rigid complexes. The light-induced electron-transfer reactions in the complexes have been studied by time-resolved absorption and emission techniques.

Experimental Section

All photophysical measurements were performed in spectroscopic-grade acetonitrile (Merck) at 298 K, unless otherwise noted. The electronic absorption spectra were recorded on a Varian Cary 50 UV−vis spectrophotometer, and steady-state emission spectra were recorded on a SPEX-Flourolog II systems flourimeter using 1-cm quartz cuvettes. Emission measurements at 77 K were performed in capillary tubes inserted in a glass dewar filled with liquid nitrogen, with butyronitrile as solvent. ^{1}H NMR spectra were recorded on a Varian 400 spectrometer.

Time-Resolved Emission Spectroscopy. The time correlated single photon counting setup was pumped with 200 kHZ pulses of 150-fs width generated in a regenerative amplified Ti:sapphire system from Coherent. The wavelength used for the experiments was 400 nm, obtained from doubling of the fundamental 800-nm light. The sample was contained in a 1 × 1 cm quartz cuvette and emission light was collected perpendicular to the incoming light. A blue filter before the sample and a monochromator after the sample was used to remove unwanted wavelengths. Emitted light was collected by a water-cooled Hammamatsu R38094-5 MCP-PMT and resulted in a response function with a fwhm of 65 ps.

Femtosecond Pump−Probe Experiments. Transient absorption pump−probe measurements were performed on a regenerative amplified Ti:sapphire system that has been described in detail previously.[28] The laser pulses generated had an average temporal width of 150 fs at 800 nm and a repetition frequency of 1 kHz. Pump light was produced in an optical parametric amplifier (TOPAS) or by simple second harmonic generation of the fundamental laser light in a BBO crystal. Before the pump light reached the sample, the remaining 800-nm light was removed with a blue filter and the intensity was set below 2 μJ with optical density filters to reduce the probability of two-photon excitation. The probe light was passed through an optical delay line followed by white light generation in a sapphire or rotating CaF_2 crystal. The white light was then focused and overlapped with the pump light in a vertically moving 1 × 10 mm sample cell. The difference in polarization between pump and probe light was adjusted with a λ/2-plate and a polarizer to obtain magic angle condition (54.7°). All the kinetic results presented are averages of five independent measurements.

Flash Photolysis. Transient absorption on a nanosecond time scale was performed with a frequency tripled Q-switched Nd:YAG laser from Quantel. The out coming light pumped an OPO delivering <10 ns flashes tunable in the range 410−660 nm. The analyzing light was provided by a pulsed 100 W Xe-lamp used in a spectrometer system from Applied Photophysics. The average energy of the laser pulses was ≅15 mJ. The concentrations of all the samples were held at ∼0.20 μM.

Mass Spectrometry. The matrix-assisted laser desorption ionization time-of-flight (MALDI-TOF) experiments were performed on a Bruker BIFLEX III spectrometer equipped with pulsed ion extraction (PIE). The spectra were taken in the reflection mode with the laser power just above the threshold of ion formation, with an accelarating voltage of 19 kV and a reflection voltage of 20 kV. 2,5-Dihydroxybenzoic acid was used as matrix, and accurate mass measurements were obtained by the use of poly(ethylene glycol) (PEG) as an external standard.

All electrospray mass spectra were aquired using a Bruker Daltonics BioAPEX-94e superconducting 9.4 T FTICR mass spectrometer (Bruker Daltonics, Billerica, MA) in broadband mode. A home-built apparatus controlled the direct infusion of sample. The sample was delivered using a helium gas container at a pressure of 1.3 bar, pushing the sample through a 30 cm fused silica capillary of inner diameter 20 μm. The sample end of the capillary was lowered into the sample tube inside the pressurized container and the electrospray end was coated by a conducting graphite/polymer layer and connected to ground.[29,30] No sheath flow or nebulizing gas was used and the flow rate was approximately 100 nL/min. The ion source was coupled to an Analytica atmosphere-vacuum interface (Analytica of Branford, CT) and a potential difference of 2−4 kV was applied across a distance of approximately 5 mm between the spraying needle and the inlet capillary.

Electrochemistry. Cyclic voltammetry and differential pulse voltammetry were carried out with a three-electrode setup in a three-compartment cell connected to an Autolab potentiostat with a GPES electrochemical interface (Eco Chemie). The working electrode was a glassy carbon disk (diameter 3 mm, freshly polished). Potentials were measured vs a nonaqueous Ag/Ag^+ reference electrode (CH Instruments, 10 mM $AgNO_3$ in acetonitrile) with a potential of −0.080 V vs the ferrocenium/ferrocene ($Fc^{+/0}$) couple in acetonitrile. All potentials reported here are referenced vs the $Fc^{+/0}$ couple by adding −0.080 V to the potentials measured vs the Ag/Ag^+ electrode.

Solutions were prepared from dry acetonitrile (Merck, spectroscopy grade, dried with MS 3 Å) and contained ca. 1 mM of the analyte and 0.1 M tetrabutylammonium hexafluorophosphate (Fluka, electrochemical grade, dried at 373 K) as supporting electrolyte. The glassware used was oven-dried, assembled, and flushed with argon while hot. Before all measurements, oxygen was removed by bubbling the stirred solutions with solvent saturated argon, and the samples were kept under argon atmosphere during measurements.

Materials. All reagents and solvents were used as received, unless otherwise noted. Pyridacylpyridinium iodide (PPI),[31] 4′-*p*-tolyl-2,2′:6′,2″-terpyridine (**8**),[32] 4-*p*-tolyl-2,2′-bipyridine (**12**),[33] 4′-(4-aminophenyl)-2,2′:6′,2″-terpyridine (**19**),[34] 4-aminomethyl-4′-methyl-2,2′-bipyridine (**20**),[35] **21**,[36] *cis*-$Ru(bpy)_2Cl_2 \cdot 2H_2O$,[37] Ru-

(28) Andersson, M.; Davidsson, J.; Hammarström, L.; Korppi-Tommola, J.; Peltola, T. *J. Phys. Chem. B* **1999**, *103*, 3258−3262.
(29) Nilsson, S.; Wetterhall, M.; Bergquist, J.; Nyholm, L.; Markides, K. *Rapid Commun. Mass Spectrom.* **2001**, *15*, 1997−2000.
(30) Wetterhall, M.; Nilsson, S.; Markides, K.; Bergquist, J. *Anal. Chem.* **2002**, *74*, 239−245.
(31) Priimov, G. U.; Moore, P.; Maritim, P. K.; Butalanyi, P. K.; Alcock, N. W. *J. Chem. Soc., Dalton Trans.* **2000**, 445−449.
(32) Neve, F.; Crispini, A.; Campagna, S.; Serroni, S. *Inorg. Chem.* **1999**, *38*, 2250−2258.
(33) Berg, K.; Tran, A.; Raymond, M. K.; Abrahamsson, M.; Wolny, J.; Andersson, M.; Sun, L.; Styring, S.; Hammarström, L.; Toftlund, H.; Åkermark, B. *Eur. J. Inorg. Chem.* **2001**, 1019−1029.
(34) Ng, W. Y.; Gong, X.; Chan, W. K. *Chem. Mater.* **1999**, *11*, 1165−1170.
(35) Hamachi, I.; Tanaka, S.; Tsukiji, S.; Shinkai, S.; Oishi, S. *Inorg. Chem.* **1998**, *37*, 4380−4388.
(36) Hayes, R. T.; Wasielewski, M. R.; Gosztola, D. *J. Am. Chem. Soc.* **2000**, *122*, 5563−5567.

$(DMSO)_4Cl_2$,[38] Ru(ttpy)(DMSO)Cl_2,[39] [Ru(ttpy)$_2$][PF_6]$_2$,[39] and Ru(tpy)Cl_3[40] were prepared as described elsewhere.

[Ru(ttpy)(ttpy-NDI)][PF_6]$_2$ (1). Compound **22** (0.100 g, 0.14 mmol) and Ru(ttpy)(DMSO)Cl_2 (0.080 g, 0.14 mmol) were added to degassed EtOH (25 mL), and the mixture was heated at reflux under nitrogen for 24 h. The solvent was removed and the residue chromatographed on silica gel (eluent: CH_3CN/H_2O/sat. KNO_3, 40:4:1). The fractions containing product were combined, and the solvent was removed. Excess KNO_3 was filtered off from a CH_3CN solution. The product was precipitated out from MeOH with an excess of NH_4PF_6 and the red solid washed with several portions of MeOH, H_2O, and Et_2O (0.067 g, 33%). ^{1}H NMR (400 MHz, [D_6]acetone, 25 °C, TMS): δ = 9.41 (s, 2H), 9.38 (s, 2H), 9.05 (d, J = 7.6 Hz, 2H), 9.01 (d, J = 8.0 Hz, 2H), 8.88 (d, J = 7.2 Hz, 2H), 8.82 (d, J = 7.6 Hz, 2H), 8.26 (d, J = 5.6 Hz, 2H), 8.24 (d, J = 5.2 Hz, 2H), 8.09 (t, J = 8.0 Hz, 4H), 7.87 (d, J = 8.4 Hz, 2H), 7.81 (d, J = 5.2 Hz, 2H), 7.78 (d, J = 5.2 Hz, 2H), 7.58 (d, J = 7.6 Hz, 2H), 7.33 (m, 4H), 5.58 (s, 2H), 4.14 (m, 2H), 2.53 (s, 3H), 2.00 (m, 1H), 1.45−1.25 (m, 8H), 0.95 (t, J = 7.2 Hz, 3H), 0.88 (3, J = 7.2 Hz, 3H). ESI-MS: m/z [M − PF_6^-]$^+$ 1269.342 (calcd for $C_{66}H_{54}N_8O_4RuPF_6$: 1269.295), [M − 2PF_6^-]$^{2+}$ 562.145 (calcd for $C_{66}H_{54}N_8O_4Ru$: 562.166). Elemental analysis calcd (%) for $C_{66}H_{54}N_8O_4RuP_2F_{12}\cdot H_2O$: C 55.35, H 3.94, N 7.82. Found: C 55.79, H 4.08, N 7.73.

[Ru(tpy)(ttpy-NDI)][PF_6]$_2$ (2). Compound **22** (0.100 g, 0.14 mmol), Ru(tpy)Cl_3 (0.063 g, 0.14 mmol), and NEt_3 (0.2 mL) were added to degassed EtOH (25 mL), and the mixture was heated at reflux under nitrogen for 18 h. The mixture was filtered while still hot, the solvent removed, and the residue chromatographed on silica gel (eluent: CH_3CN/H_2O/sat. KNO_3, 40:4:1). Fractions containing product were combined and the solvent removed. Excess KNO_3 was filtered off from a CH_3CN solution. The product was precipitated out from MeOH with an excess of NH_4PF_6 and the red solid washed with several portions of MeOH, H_2O, and Et_2O (0.066 g, 35%). ^{1}H NMR (400 MHz, [D_6]acetone, 25 °C, TMS): δ = 9.38 (s, 2H), 9.09 (d, J = 8.0 Hz, 2H), 9.00 (d, J = 7.6 Hz, 2H), 8.87 (d, J = 7.6 Hz, 2H), 8.82 (d, J = 7.6 Hz, 4H), 8.58 (t, J = 8.4 Hz, 1H), 8.25 (d, J = 8.4 Hz, 2H), 8.07 (m, 4H), 7.87 (d, J = 8.4 Hz, 2H), 7.77 (d, J = 4.8 Hz, 2H), 7.71 (d, J = 4.8 Hz, 2H), 7.32 (m, 4H), 5.58 (s, 2H), 4.14 (m, 2H), 1.44−1.24 (m, 8H), 0.95 (t, J = 7.6 Hz, 3H), 0.90 (t, J = 7.2 Hz), −CH− proton hidden under solvent peak. ESI-MS: m/z [M − PF_6^-]$^+$ 1179.246 (calcd for $C_{59}H_{48}N_8O_4RuPF_6$: 1179.248), [M − 2PF_6^-]$^{2+}$ 517.142 (calcd for $C_{59}H_{48}N_8O_4Ru$: 517.142). Elemental analysis calcd (%) for $C_{59}H_{48}N_8O_4RuP_2F_{12}\cdot H_2O$: C 52.80, H 3.76, N 8.35. Found: C 52.62, H 3.89, N 8.22.

[Ru(ttpy)(phtpy-NDI)][PF_6]$_2$ (3). This complex was prepared as **1** above, by refluxing compound **23** (0.090 g, 0.13 mmol) and Ru(ttpy)(DMSO)Cl_2 (0.072 g, 0.13 mmol) in EtOH (25 mL) for 16 h (0.055 g, 31%). ^{1}H NMR (400 MHz, CD_3CN, 25 °C, TMS): δ = 9.12 (s, 2H), 9.02 (s, 2H), 8.79 (d, J = 7.2 Hz, 2H), 8.78 (d, J = 7.6 Hz, 2H), 8.68 (d, J = 7.6 Hz, 2H), 8.66 (d, J = 8.0 Hz, 2H), 8.38 (d, J = 8.4 Hz, 2H), 8.12 (d, J = 8.0 Hz, 2H), 8.00−7.94 (m, 4H), 7.79 (d, J = 8.4 Hz, 2H), 7.59 (d, J = 8.0 Hz, 2H), 7.46 (d, J = 5.6 Hz, 4H), 7.20 (t, J = 6.0 Hz, 4H), 4.12 (m, 2H), 2.55 (s, 3H), 1.50−1.30 (m, 8H), 0.96 (t, J = 7.2 Hz, 3H), 0.90 (t, J = 7.2 Hz, 3H), −CH− proton hidden under solvent peak. ESI-MS: m/z [M − PF_6^-]$^+$ 1255.318 (calcd for $C_{65}H_{52}N_8O_4RuPF_6$: 1255.280), [M − 2PF_6^-]$^{2+}$ 555.137 (calcd for $C_{65}H_{52}N_8O_4Ru$: 555.158), minor peak at 1172.306 (calcd for $C_{65}H_{52}N_8O_4RuNO_3$: 1172.303). Elemental analysis calcd (%) for $C_{65}H_{52}N_8O_4RuP_2F_{12}$: C 55.76, H 3.74, N 8.00. Found: C 56.59, H 4.04, N 9.34.

[Ru(tpy)(phtpy-NDI)][PF_6]$_2$ (4). This complex was prepared as **2** above, by refluxing compound **23** (0.056 g, 0.08 mmol), Ru(tpy)Cl_3 (0.031 g, 0.07 mmol), and NEt_3 (0.1 mL) in EtOH (20 mL) for 18 h (0.042 g, 46%). ^{1}H NMR (400 MHz, CD_3CN, 25 °C, TMS): δ = 9.10 (s, 2H), 8.79 (d, J = 7.6 Hz, 2H), 8.77 (d, J = 7.2 Hz, 2H), 8.76 (d, J = 8.0 Hz, 2H), 8.65 (d, J = 7.6 Hz, 2H), 8.51 (d, J = 7.6 Hz, 2H), 8.42 (t, J = 8.0 Hz, 1H), 8.37 (d, J = 8.4 Hz, 2H), 7.96 (dt, J = 7.6, 1.2, 2H), 7.94 (dt, J = 8.0, 1.2 Hz, 2H), 7.79 (d, J = 8.4 Hz, 2H), 7.45 (dd, J = 4.8, 0.8 Hz, 2H), 7.37 (dd, J = 4.8, 0.8 Hz, 2H), 7.22−7.16 (m, 4H), 4.12 (m, 2H), 1.50−1.30 (m, 8H), 0.96 (t, J = 7.2 Hz, 3H), 0.90 (t, J = 7.6 Hz, 3H), −CH− proton hidden under solvent peak. ESI-MS: m/z [M − PF_6^-]$^+$ 1165.216 (calcd for $C_{58}H_{46}N_8O_4RuPF_6$: 1165.233), [M − 2PF_6^-]$^{2+}$ 510.137 (calcd for $C_{58}H_{46}N_8O_4Ru$: 510.134). Elemental analysis calcd (%) for $C_{58}H_{46}N_8O_4RuP_2F_{12}$: C 53.18, H 3.54, N 8.55. Found: C 52.92, H 3.66, N 8.38.

[Ru(bpy)$_2$(bpy-NDI)][PF_6]$_2$ (5). Compound **26** (0.100 g, 0.18 mmol) and Ru(bpy)$_2Cl_2\cdot 2H_2O$ (0.090 g, 0.17 mmol) were added to degassed EtOH (30 mL), and the solution was heated at reflux under nitrogen in the dark for 19 h. The solvent was removed and the residue chromatographed on silica gel (eluent: CH_3CN/H_2O/sat. KNO_3, 40:4:1). Fractions containing product were combined, and the solvent was removed. H_2O, CH_2Cl_2, and an excess of NH_4PF_6 were added, and the mixture was left stirring. The organic phase was separated, washed with additional H_2O, and dried, and the solvent was removed to give **5** (0.198 g, 87%). ^{1}H NMR (400 MHz, CD_3CN, 25 °C, TMS): δ = 8.72 (s, 4H), 8.50−8.42 (m, 5H), 8.35 (s, 1H), 8.07−7.98 (m, 4H), 7.74−7.66 (m, 4H), 7.64 (d, J = 6.0 Hz, 1H), 7.51 (d, J = 5.6 Hz, 1H), 7.43 (dd, J = 6.0, 1.6 Hz, 1H), 7.40−7.33 (m, 4H), 7.21 (d, J = 4.0 Hz, 1H), 5.46 (s, 2H), 4.08 (m, 2H), 2.46 (s, 3H), 1.44−1.26 (m, 8H), 0.93 (t, J = 7.6 Hz, 3H), 0.88 (t, J = 7.2 Hz, 3H), −CH− proton hidden under solvent peak. ESI-MS: m/z [M − PF_6^-]$^+$ 1119.248 (calcd for $C_{54}H_{48}N_8O_4RuPF_6$: 1119.248). Elemental analysis calcd (%) for $C_{54}H_{48}N_8O_4RuP_2F_{12}$: C 51.31, H 3.83, N 8.86. Found: C 51.16, H 3.99, N 8.70.

[Ru(bpy)$_2$(phbpy-NDI)][PF_6]$_2$ (6). This complex was prepared as **5** above, by refluxing compound **25** (0.061 g, 0.10 mmol) and Ru(bpy)$_2Cl_2\cdot 2H_2O$ (0.050 g, 0.10 mmol) in EtOH (20 mL) for 8 h (0.095 g, 75%). ^{1}H NMR (400 MHz, CD_3CN, 25 °C, TMS): δ = 8.84 (d, 1H, J = 2.0 Hz), 8.75 (d, J = 7.6 Hz, 2H), 8.71 (d, 7.6 Hz, 2H), 8.70 (d, J = 8.0 Hz, 1H), 8.55−8.49 (m, 4H), 8.12−8.02 (m, 7H), 7.82−7.72 (m, 7H), 7.62 (d, J = 8.8 Hz, 2H), 7.46−7.40 (m, 5H), 4.10 (m, 2H),1.50−1.30 (m, 8H), 0.95 (t, J = 7.2 Hz, 3H), 0.89 (t, J = 7.2 Hz, 3H), −CH− proton hidden under solvent peak. ESI-MS: m/z [M − PF_6^-]$^+$ 1167.234 (calcd for $C_{58}H_{48}N_8O_4RuPF_6$: 1167.248), [M − 2PF_6^-]$^{2+}$ 511.137 (calcd for $C_{58}H_{48}N_8O_4Ru$: 511.142). Elemental analysis calcd (%) for $C_{58}H_{48}N_8O_4RuP_2F_{12}$: C 53.09, H 3.69, N 8.54. Found: C 52.93, H 3.87, N 8.44.

[Ru(bpy)$_2$(tbpy-NDI)][PF_6]$_2$ (7). This complex was prepared as **5** above, by refluxing compound **24** (0.110 g, 0.18 mmol) and Ru(bpy)$_2Cl_2\cdot 2H_2O$ (0.090 g, 0.17 mmol) in EtOH (30 mL) for 45 h (0.173 g, 77%). ^{1}H NMR (400 MHz, CD_3CN, 25 °C, TMS): δ = 8.72 (d, J = 7.6 Hz, 2H), 8.70 (s, 1H), 8.69 (d, J = 7.6 Hz, 2H), 8.64 (d, J = 8.4 Hz, 1H), 8.52−8.46 (m, 4H), 8.08−8.02 (m,

(37) Lay, P. A.; Sargeson, A. M.; Taube, H. *Inorg. Synth.* **1986**, *24*, 291−299.
(38) Evans, I. P.; Spencer, A.; Wilkinson, G. *J. Chem. Soc., Dalton Trans.* **1973**, 204−209.
(39) Norrby, T.; Börje, A.; Åkermark, B.; Hammarström, L.; Alsins, J.; Lashgari, K.; Norrestam, R.; Mårtensson, J.; Stenhagen, G. *Inorg. Chem.* **1997**, *36*, 5850−5858.
(40) Sullivan, B. P.; Calvert, J. M.; Meyer, T. J. *Inorg. Chem.* **1980**, *19*, 1404−1407.

5H), 7.82 (d, $J = 8.8$ Hz, 2H), 7.78−7.72 (m, 5H), 7.70 (d, $J = 6.0$ Hz, 1H), 7.65 (d, $J = 8.4$ Hz, 2H), 7.61 (dd, $J = 6.0$, 2.0 Hz, 1H), 7.42−7.36 (m, 5H), 5.42 (s, 2H), 4.07 (m, 2H), 1.44−1.26 (m, 8H), 0.93 (t, $J = 7.2$ Hz, 3H), 0.87 (t, $J = 7.2$ Hz, 3H), −CH− proton hidden under solvent peak. ESI-MS: m/z $[M - PF_6^-]^+$ 1181.271 (calcd for $C_{59}H_{50}N_8O_4RuPF_6$: 1181.264). Elemental analysis calcd (%) for $C_{59}H_{50}N_8O_4RuP_2F_{12}$: C 53.44, H 3.80, N 8.45. Found: C 53.25, H 3.82, N 8.47.

4′-(4-Bromomethylphenyl)-2,2′:6′,2″-terpyridine (9). 4′-*p*-Tolyl-2,2′:6′,2″-terpyridine (**8**) (2.00 g, 6.18 mmol), *N*-bromosuccinimide (1.12 g, 6.29 mmol), and azobisisobutyronitrile (0.033 g) were added to degassed CCl_4 (40 mL), and the mixture was heated at reflux under nitrogen for 3 h. The yellow cloudy solution was allowed to cool to room temperature and filtered, the solvent removed, and the remaining solid recrystallized from an acetone/EtOH mixture (1:2) to give **9** as a white solid (1.73 g, 70%). ^{1}H NMR (400 MHz, $CDCl_3$, 25 °C, TMS): $\delta = 8.73$ (m, 4H), 8.67 (d, $J = 8.0$ Hz, 2H), 7.88 (m, 4H), 7.54 (d, $J = 8.0$ Hz, 2H), 7.35 (ddd, $J = 7.6$, 4.8, 0.8 Hz, 2H), 4.57 (s, 2H).

4′-(4-Phthalimidomethylphenyl)-2,2′:6′,2″-terpyridine (10). Compound **9** (0.50 g, 1.25 mmol) and potassium phthalimide (0.24 g, 1.31 mmol) were added to DMF (15 mL), and the mixture was heated at 80 °C for 4.5 h. The mixture was left at room temperature overnight. H_2O (30 mL) was added and the resulting solid was filtered off and washed with several portions of H_2O and Et_2O (0.45 g, 76%). ^{1}H NMR (400 MHz, $CDCl_3$, 25 °C, TMS): $\delta = 8.71$ (m, 2H), 8.70 (s, 2H), 8.65 (d, $J = 8.0$ Hz, 2H), 7.88−7.84 (m, 6H), 7.72 (m, 2H), 7.58 (d, $J = 8.0$ Hz, 2H), 7.34 (ddd, $J = 7.6$, 4.8, 1.2 Hz, 2H), 4.93 (s, 2H).

4′-(4-Aminomethylphenyl)-2,2′:6′,2″-terpyridine (11). Compound **10** (0.44 g, 0.95 mmol) and hydrazine (55%, 0.3 mL, 5 mmol) were added to a $CHCl_3$/EtOH mixture (1:1.5, 25 mL) and heated at reflux for 8 h under nitrogen. $CHCl_3$ was added (25 mL) and the mixture was filtered, leaving behind a white solid. The filtrate was washed with H_2O, NaOH (1 M), and an additional time with H_2O. The organic phase was dried over Na_2SO_4 and the solvent removed to give **11** as a white solid (0.27 g, 84%). ^{1}H NMR (400 MHz, $CDCl_3$, 25 °C, TMS): $\delta = 8.73$ (br s, 4H), 8.67 (d, $J = 8.0$ Hz, 2H), 7.88 (m, 4H), 7.46 (d, $J = 8.0$ Hz, 2H), 7.35 (m, 2H), 3.96 (s, 2H), 1.70 (br s, 2H).

4-(4-Bromomethylphenyl)-2,2′-bipyridine (13). This was prepared as described by Berg et al.[33] by a modified procedure. 4-*p*-Tolyl-2,2′-bipyridine (**12**) (1.04 g, 4.2 mmol), *N*-bromosuccinimide (0.76 g, 4.3 mmol), and benzoyl peroxide (0.049 g) were added to degassed CCl_4 (50 mL), and the mixture was heated at reflux under nitrogen for 5 h. The formed succinimide was filtered off and the solvent removed to give a yellow solid. This was recrystallized from an EtOH/acetone mixture (3:1) to give **13** as a slightly yellow solid (0.76 g, 56%). ^{1}H NMR (400 MHz, $CDCl_3$, 25 °C, TMS): $\delta = 8.73$ (d, $J = 5.2$ Hz, 1H), 8.71 (m, 1H), 8.67 (d, $J = 1.2$ Hz, 1H), 8.45 (d, $J = 8.0$ Hz, 1H), 7.84 (dt, $J = 7.6$, 1.6 Hz, 1H), 7.75 (d, $J = 8.0$ Hz, 2H), 7.53 (m, 3H), 7.33 (ddd, $J = 7.2$, 4.8, 0.8 Hz, 1H), 4.56 (s, 2H).

4-(4-Phthalimidomethylphenyl)-2,2′-bipyridine (14). Compound **13** (0.74 g, 2.29 mmol) and potassium phthalimide (0.45 g, 2.43 mmol) were added to dry DMF (30 mL), and the solution was stirred for 5 h at 85 °C. After cooling to room temperature, H_2O (60 mL) and $CHCl_3$ (40 mL) were added. The organic phase was separated and the H_2O phase extracted with additional $CHCl_3$. The combined organic phase was washed with brine and H_2O and dried over Na_2SO_4, and the solvent was removed to give **14** (0.83 g, 92%). ^{1}H NMR (400 MHz, $CDCl_3$, 25 °C, TMS): $\delta = 8.72$−8.68 (m, 2H), 8.63 (m, 1H), 8.43 (d, $J = 8.0$ Hz, 1H), 7.87 (m, 2H), 7.83 (dt, $J = 7.6$, 1.6 Hz, 1H), 7.74−7.70 (m, 4H), 7.56 (d, $J = 8.0$ Hz, 2H), 7.49 (dd, $J = 5.2$, 1.6 Hz, 1H), 7.32 (ddd, $J = 7.2$, 4.8, 0.8 Hz, 1H), 4.92 (s, 2H).

4-(4-Aminomethylphenyl)-2,2′-bipyridine (15). Compound **14** (0.74 g, 1.90 mmol) and hydrazine (55%, 0.35 mL, 6 mmol) were added to EtOH (30 mL), and the mixture was heated at reflux for 7 h. NaOH (1 M, 50 mL) was added and the mixture extracted with $CHCl_3$. The organic phase was washed with H_2O and dried over Na_2SO_4. The solvent was removed to give **15** as a slightly yellow solid (0.46 g, 92%). ^{1}H NMR (400 MHz, $CDCl_3$, 25 °C, TMS): $\delta = 8.74$−8.70 (m, 2H), 8.67 (d, $J = 2.0$ Hz, 1H), 8.45 (d, $J = 8.0$ Hz, 1H), 7.84 (dt, $J = 7.6$, 1.6 Hz, 1H), 7.60 (d, $J = 8.0$ Hz, 2H), 7.54 (dd, $J = 4.8$, 2.0 Hz, 1H), 7.45 (d, $J = 8.0$ Hz, 2H), 7.33 (dd, $J = 7.6$, 4.8 Hz, 1H), 3.95 (s, 2H).

(*E*)-4-(4-Nitrophenyl)-2-oxo-3-butenoic Acid (16). 4-Nitrobenzaldehyde (4.13 g, 27.33 mmol) was added to EtOH (50 mL) and the mixture was heated at 70 °C until all dissolved. Sodium pyruvate (3.10 g, 28.17 mmol) dissolved in H_2O (15 mL) was added and the mixture was cooled on ice. NaOH (0.5 M, 25 mL) was added dropwise, and the mixture was left on ice for an additional 2.5 h. The mixture was neutralized with HCl (2 M) and filtered, and the remaining solid was washed with EtOH and air-dried (3.60 g, 60%). ^{1}H NMR (400 MHz, $[D_6]$DMSO, 25 °C, TMS): $\delta = 8.22$ (d, $J = 8.8$ Hz, 2H), 7.94 (d, $J = 8.8$ Hz, 2H), 7.50 (d, $J = 16.4$ Hz, 1H), 6.96 (d, $J = 16.8$ Hz, 1H).

4-(4-Nitrophenyl)-2,2′-bipyridine (17). Compound **16** (2.98 g, 13.5 mmol), pyridacyl pyridinium iodide (4.40 g, 13.5 mmol), and NH_4OAc (8.3 g, 108 mmol) were added to H_2O (90 mL), and the suspension was heated at reflux for 5 h. The formed solid was filtered off and washed with H_2O and acetone to give the ammonium salt of 4-(4-nitrophenyl)-6-carboxylate-2,2′-bipyridine (3.60 g, 79%).

The ammonium salt (1.33 g, 3.93 mmol) was heated under vacuum with a heatgun until the evolution of CO_2 ceased. After cooling, the formed black solid was dissolved in EtOAc, activated charcoal was added, and the mixture was refluxed for 15 min. After filtration through Celite, the solvent was removed to give **17** as a slightly yellow solid (0.81 g, 58%, total yield). ^{1}H NMR (400 MHz, $[D_6]$DMSO, 25 °C, TMS): $\delta = 8.84$ (dd, $J = 5.2$, 0.8 Hz, 1H), 8.56−8.52 (m, 2H), 8.45 (dd, $J = 8.0$, 0.8 Hz, 1H), 8.39 (d, $J = 8.8$ Hz, 2H), 8.17 (d, $J = 8.8$ Hz, 2H), 8.00 (dt, $J = 8.0$, 2.0 Hz, 1H), 7.89 (dd, $J = 4.8$, 1.6 Hz, 1H), 7.51 (ddd, $J = 7.6$, 4.8, 0.8 Hz, 1H).

4-(4-Aminophenyl)-2,2′-bipyridine (18). Compound **17** (0.80 g, 2.85 mmol) and 10% Pd/C (0.30 g) were added to EtOH (30 mL), and the mixture was refluxed for 1 h. H_2NNH_2 (55%, 3.5 mL, ∼20 equiv) was added and the mixture was refluxed for another hour. The mixture was filtered through Celite and the solid washed with additional CH_2Cl_2. H_2O was added and the organic phase was separated and washed with additional H_2O. After drying over Na_2SO_4, the solvent was removed to give **18** as a white solid (0.62 g, 88%). ^{1}H NMR (400 MHz, $CDCl_3$, 25 °C, TMS): $\delta = 8.70$ (m, 1H), 8.65 (d, $J = 5.2$ Hz, 1H), 8.61 (d, $J = 1.2$ Hz, 1H), 8.43 (d, $J = 8.0$ Hz, 1H), 7.83 (dt, $J = 7.6$, 1.6 Hz, 1H), 7.63 (d, $J = 8.8$ Hz, 2H), 7.49 (dd, $J = 5.2$, 1.6 Hz, 1H), 7.32 (ddd, $J = 7.6$, 5.2, 1.2 Hz, 1H), 6.78 (d, $J = 8.8$ Hz, 2H), 3.86 (s, 2H).

Compound 22. Compounds **11** (0.26 g, 0.76 mmol) and **21** (0.40 g, 1.05 mmol) were suspended in freshly distilled toluene (50 mL), and the mixture was heated at reflux under nitrogen for 12 h. The mixture was cooled to room temperature and filtered, and the resulting solid was washed with several portions of cold toluene and petroleum ether (0.35 g, 65%). There is substantial line broadening in the NMR spectrum due to the insolubility of the

compound. ^{1}H NMR (400 MHz, $CDCl_3$, 25 °C, TMS): δ = 8.82−8.75 (m, 4H), 8.70−8.62 (m, 6H), 7.86 (s, 4H), 7.70 (d, 2H), 7.34 (s, 2H), 5.48 (s, 2H), 4.13 (m, 2H), 1.94 (s, 1H), 1.45−1.20 (m, 8H), 1.00−0.80 (m, 6H). MS (MALDI-TOF): found $[M + H^+]^+$ 700.3 *m*/*z* (calcd for $C_{44}H_{38}N_5O_4$: 700.3).

Compound 23. Compounds **19** (0.23 g, 0.70 mmol) and **21** (0.26 g, 0.70 mmol) were dissolved in freshly distilled *N*,*N*-dimethylacetamide (20 mL), and the solution was heated at reflux under argon for 19 h. The temperature was reduced to 80 °C, freshly distilled acetic anhydride (10 mL) and pyridine (5 mL) were added, and the solution was left for another 20 h at this temperature. The reaction mixture was cooled to room temperature and poured into H_2O (50 mL). The aqueous phase was extracted with CH_2Cl_2, and the organic phase was washed with H_2O and brine. After drying and removal of solvent, the residue was chromatographed on silica (eluent: CH_2Cl_2) to give **23** (0.21 g, 45%). ^{1}H NMR (400 MHz, $CDCl_3$, 25 °C, TMS): δ = 8.84 (s, 2H), 8.82 (d, J = 7.2 Hz, 2H), 8.79 (d, J = 7.6 Hz, 2H), 8.76 (d, J = 4.8 Hz, 2H), 8.71 (d, J = 7.6 Hz, 2H), 8.14 (d, J = 8.4 Hz, 2H), 7.93 (t, J = 7.6 Hz, 2H), 7.50 (d, J = 8.4 Hz, 2H), 7.40 (dd, J = 6.8, 5.2 Hz, 2H), 4.16 (m, 2H), 1.96 (m, 1H), 1.45−1.25 (m, 8H), 0.96 (t, J = 7.2 Hz, 3H), 0.89 (t, J = 7.2 Hz, 3H). MS (MALDI-TOF): found $[M + H^+]^+$ 686.3 *m*/*z* (calcd for $C_{43}H_{36}N_5O_4$: 686.3).

Compound 24. This ligand was prepared as **22** above. Compounds **15** (0.20 g, 0.77 mmol) and **21** (0.31 g, 0.82 mmol) gave **24** (0.30 g, 63%). The NMR spectrum gave sharp signals as compared to the analogous terpyridinediimide ligand **22**. ^{1}H NMR (400 MHz, $CDCl_3$, 25 °C, TMS): δ = 8.80 (d, J = 7.6 Hz, 2H), 8.76 (d, J = 7.6 Hz, 2H), 8.70−8.66 (m, 2H), 8.62 (d, J = 1.2 Hz, 1H), 8.42 (d, J = 8.0 Hz, 1H), 7.82 (dt, J = 8.0, 2.0 Hz, 1H), 7.73 (d, J = 8.0 Hz, 2H), 7.68 (d, J = 8.0 Hz, 2H), 7.48 (dd, J = 5.2, 1.2 Hz, 1H), 7.31 (dd, J = 7.6, 4.8 Hz, 1H), 5.46 (s, 2H), 4.14 (m, 2H), 1.94 (m, 1H), 1.45−1.20 (m, 8H), 0.93 (t, J = 7.2 Hz, 3H), 0.87 (t, J = 7.2 Hz, 3H). MS (MALDI-TOF): found $[M + H^+]^+$ 623.4 *m*/*z* (calcd for $C_{39}H_{35}N_4O_4$: 623.3).

Compound 25. This ligand was prepared as **23** above. Compounds **18** (1.07 g, 4.32 mmol) and **21** (1.64 g, 4.32 mmol) gave **25** (1.45 g, 55%). ^{1}H NMR (400 MHz, $CDCl_3$, 25 °C, TMS): δ = 8.83 (d, J = 7.6 Hz, 2H), 8.80 (d, J = 7.6 Hz, 2H), 8.79 (d, J = 4.8 Hz, 1H), 8.75 (m, 1H), 8.73 (d, J = 0.8 Hz, 1H), 8.46 (d, J = 8.0 Hz, 1H), 7.98 (d, J = 8.4 Hz, 2H), 7.87 (dt, J = 7.6, 1.6 Hz, 1H), 7.62 (dd, J = 5.2, 2.0 Hz, 1H), 7.48 (d, J = 8.4 Hz, 2H), 7.36 (ddd, J = 7.6, 4.8, 1.2 Hz, 1H), 4.17 (m, 2H), 1.96 (m, 1H), 1.45−1.25 (m, 8H), 0.96 (t, J = 7.6 Hz, 3H), 0.89 (t, J = 7.2 Hz, 3H). MS (MALDI-TOF): found $[M + H^+]^+$ 609.4 *m*/*z* (calcd for $C_{38}H_{33}N_4O_4$: 609.3).

Compound 26. This ligand was prepared as **22** above. Compounds **20** (0.15 g, 0.76 mmol) and **21** (0.30 g, 0.79 mmol) gave **26** (0.29 g, 68%). The NMR spectrum seemed to give a mixture of at least two species in $CDCl_3$ and $[D_6]$DMSO independent of concentration. This is believed to be caused by some stacking effect. MS (MALDI-TOF): found $[M + H^+]^+$ 561.4 *m*/*z* (calcd for $C_{34}H_{33}N_4O_4$: 561.3).

Results

Synthesis and Characterization. The new polypyridine terpyridine and bipyridine based ruthenium complexes **1**−**7** (Figure 1) were prepared from monoterpyridine ruthenium(II), monoterpyridine ruthenium(III), or bisbipyridine ruthenium(II) precursors and the appropriate functionalized terpyridine or bipyridine ligands **22**−**26**. These ligands, in turn, were prepared by the reaction of the anhydride **21**[36] and the aminoterpyridines **11** and **19**[34] or the aminobipyridines **15**, **18**, and **20**[35] (Scheme 2). As might be anticipated, the amines **18** and **19** were unreactive, and fairly forcing conditions had to be employed in the preparation of diimides **23** and **25**. The aminoterpyridine **11** and the aminobipyridine **15** were both prepared by functionalization of the methyl groups of **8**[32] and **12**,[33] respectively. The aminobipyridine **18** was synthesized via the chalcone **16** and PPI (Scheme 1).[31]

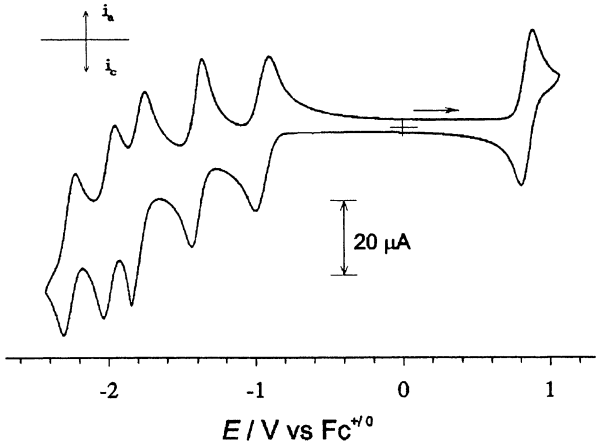

Figure 2. Cyclic voltammogram of **5** (1 mM) in CH_3CN with 0.1 M $N(n\text{-}C_4H_9)_4PF_6$. υ = 0.100 V s^{-1}.

The complexes **1**−**7** could be fully characterized by ^{1}H NMR spectroscopy, electrospray mass spectrometry, and elemental analysis. It is interesting to note that among the ligands **22**−**26**, only **23**−**25** gave nice NMR spectra. In contrast, the compound **22** gave broad signals and **26** behaved as if composed of two different structures, as indicated by two sets of bipyridine resonances. The reason could be association in solution. All ligands showed the $[M + H^+]^+$ peak in the MALDI-TOF mass spectrometry.

Electrochemistry. The electrochemical properties of complexes **1**−**7** were studied by cyclic voltammetry (CV) and differential pulse voltammetry (DPV). The CV of complex **5** showed six reversible to quasiresversible waves (Figure 2), while the other complexes were adsorbed to the electrode after reduction to neutral overall charge. Where CV waves were perturbed by these effects, half-wave potentials were determined from DPV peak potentials (Table 1). From comparisons with $[Ru(bpy)_3]^{2+}$ and NDI, the peaks in Figure 2 can be assigned to oxidation of the ruthenium moiety, two reductions of the NDI moiety, and three reductions of the bipyridine ligands. In none of the complexes **1**−**7** is there any substantial effect of the electron-withdrawing NDI unit on the oxidation potential of the ruthenium moiety. Also, the first reduction potential of the NDI moiety is only slightly affected by the ruthenium moiety, suggesting that the interaction between the two is limited. This is also suggested by the UV−vis absorption data below.

Absorption Properties. In Table 2, absorption maxima and intensities are reported for complexes **1**−**7**. For all complexes, the absorption spectra observed closely match the sum of the spectra for the $[Ru(bpy)_3]^{2+}$ and NDI units, indicating that the electronic interaction between the acceptor

Scheme 1[a]

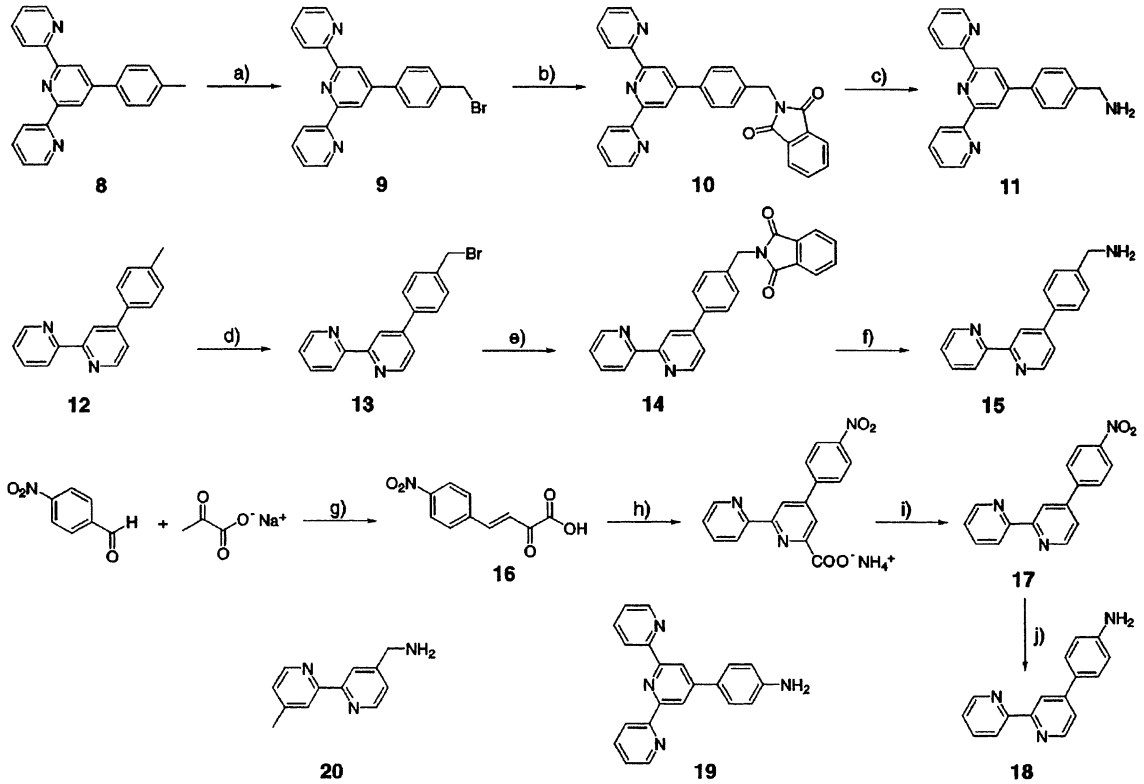

[a] (a) NBS, AIBN, CCl_4, reflux (70%); (b) potassium phthalimide, DMF, 80 °C (76%); (c) H_2NNH_2, EtOH/$CHCl_3$, reflux (84%); (d) NBS, benzoyl peroxide, CCl_4, reflux (56%); (e) potassium phthalimide, DMF, 85 °C (92%); (f) H_2NNH_2, EtOH, reflux (92%); (g) EtOH/H_2O, OH^-, 0 °C (60%); (h) PPI, NH_4OAc, H_2O, reflux (79%); (i) heat (74%), (j) H_2NNH_2, Pd/C, EtOH, reflux (88%). 4′-(4-Aminophenyl)-2,2′:6′,2″-terpyridine (**19**) and 4-aminomethyl-4′-methyl-2,2′-bipyridine (**20**) were prepared as described elsewhere.[34,35]

Scheme 2[a]

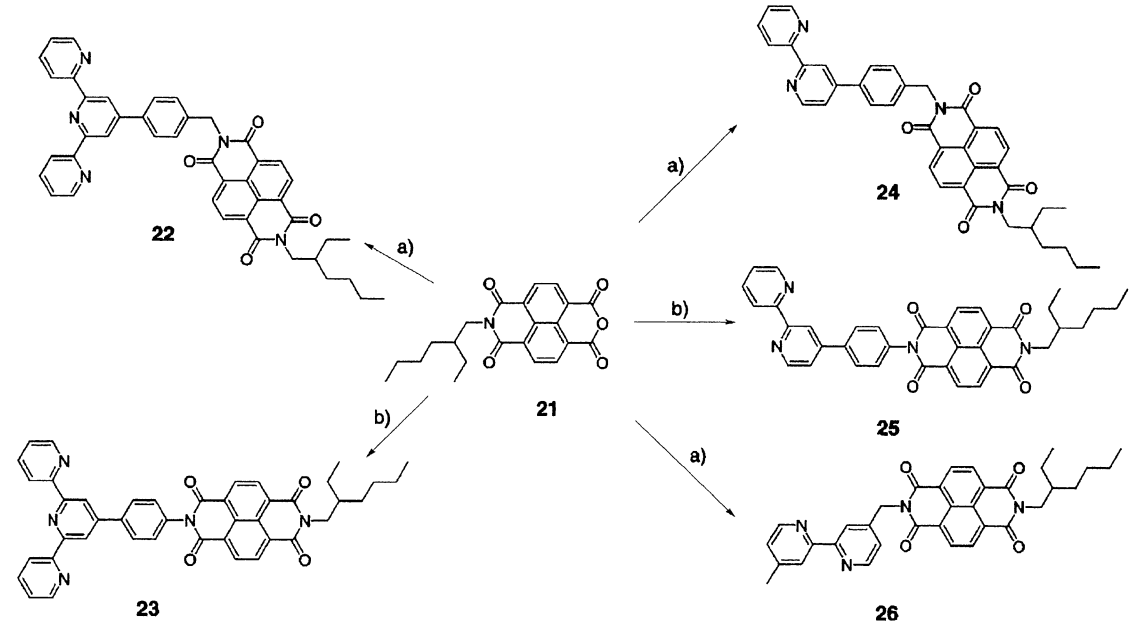

[a] (a) For **22**, **24**, **26**: toluene, reflux with appropriate oligopyridine 12 h (65%, 63%, 68%, respectively); (b) For **23** and **25**: DMA, reflux with appropriate oligopyridine 20 h, addition of Ac_2O and pyridine 12 h (45% and 55%).

and the chromophore is small. This supports the idea that the NDI is twisted out of the plane of the phenyl ring for **3**, **4**, and **6**.

The metal-to-ligand charge-transfer absorption of the terpyridine complexes **1** and **3** has higher intensity than **2** and **4**. This is an effect of delocalization of the MLCT state on the tolyl group, increasing the transition dipole moment in the former complexes.[8,10,41,42] The same effect was observed in the corresponding bipyridine complexes **6** and **7**.

Emission Properties. The emission maxima and lifetimes of complexes **1**−**7**, together with the parent complexes $[Ru(ttpy)_2]^{2+}$ and $[Ru(bpy)_3]^{2+}$, are presented in Table 3. Time-

Table 1. Electrochemical Data of Complexes **1**−**7** and Model Complexes

	$E_{1/2}$/V[b] (ΔE_p/mV)[c]						
complex[a]	$[Ru(xpy)_2]^{-/2-}$	$[Ru(xpy)_2]^{0/-}$	$[Ru(xpy)_2]^{+/0}$	$[Ru(xpy)_2]^{2+/+}$	$NDI^{-/2-}$	$NDI^{0/-}$	$[Ru(xpy)_2]^{3+/2+}$
$[Ru(ttpy)_2]^{2+}$	−2.685 (162)	−2.340 (121)	−1.895 (111)	−1.650 (112)			−0.835 (117)
1	−2.680[d] (−)[e]	−2.325[d] (−)[e]	−1.950[d] (−)[e]	−1.690[d] (−)[e]	−1.380[d] (−)[e]	−0.970[d] (−)[e]	−0.850 (107)
2	−2.740[d] (−)[e]	−2.325[d] (−)[e]	−1.925[d] (−)[e]	−1.765[d,f] (−)[e]	−1.365[d] (−)[e]	−0.970 (105)	−0.875 (109)
3	−2.675[d] (−)[e]	−2.325[d] (−)[e]	−1.920[d] (−)[e]	−1.770[d] (−)[e]	−1.310[d] (−)[e]	−0.970 (107)	−0.860 (108)
4	−2.730[d] (−)[e]	−2.340[d] (−)[e]	−1.935[d] (−)[e]	−1.730[d] (−)[e]	−1.335[d] (−)[e]	−0.970 (104)	−0.880 (100)
$[Ru(bpy)_3]^{2+}$	−2.665 ()[g]	−2.180 (80)	−1.930 (68)	−1.740 (76)			−0.880 (79)
5	−2.840 ()[g]	−2.265 (77)	−1.995 (85)	−1.795 (97)	−1.400 (72)	−0.955 (100)	−0.850 (82)
6	−2.745[d] (−)[e]	−2.155[d] (−)[e]	−1.910[d] (−)[e]	−1.730[d] (−)[e]	−1.370[d] (−)[e]	−0.975 (78)	−0.870 (74)
7	−2.745[d] (−)[e]	−2.135[d] (−)[e]	−1.920[d] (−)[e]	−1.725[d] (−)[e]	−1.365[d] (−)[e]	−0.965 (70)	−0.875 (64)

[a] As PF_6^- salts. [b] Versus Fc^+/Fc, in CH_3CN solution with 0.1 M $[N(n\text{-}C_4H_9)_4]PF_6$ as supporting electrolyte, ±0.02 V. [c] $\upsilon = 100$ mV s^{-1}. [d] DPV peak potential. [e] CV peak or counter-peak perturbed by adsorption to the electrode. [f] DPV shoulder. [g] Irrevesible CV wave.

Table 2. UV−Visible Spectral Data of Complexes **1**−**7** and Model Complexes

	λ_{max}/nm ($\epsilon \times 10^4$/M^{-1} cm^{-1})	
complex[a]	d → π^*	$\pi \rightarrow \pi^*$
$[Ru(ttpy)_2]^{2+}$ [8]	490 (2.8)	310 (7.6), 284 (6.8)
1	490 (3.2)	379 (3.2), 358 (2.9), 311 (8.2), 285 (7.6), 235 (7.1)
2	483 (2.3)	379 (3.1), 358 (2.8), 308 (7.5), 283 (5.2), 274 (5.1), 235 (6.7)
3[b]	490 (3.4)	378 (3.7), 357 (3.5), 311 (8.3), 285 (8.2), 235 (7.7)
4	483 (2.5)	378 (3.6), 357 (3.3), 309 (7.6), 282 (5.8), 274 (5.7), 235 (7.3)
$[Ru(bpy)_3]^{2+}$ [c]	451 (1.4)	288 (7.9), 254 (sh, 2.1), 244 (2.4)
5	455 (1.4)	379 (3.1), 358 (2.7), 340 (1.9), 287 (7.9), 236 (5.1)
6	456 (1.7)	378 (3.6), 358 (3.2), 339 (2.4), 288 (8.6), 236 (5.9)
7	456 (1.7)	379 (3.4), 359 (3.0), 340 (2.3), 289 (8.2), 237 (5.7)

[a] As PF_6^- salts. [b] Mixture of counterions. [c] Anderson et al. *Inorg. Chem.* **1995**, *34*, 6145−6157.

Table 3. Photophysical Data of Complexes **1**−**7** and Model Complexes

complex[a]	Ems (77 K) (nm)	E_{00}[b] (eV)	E_{CS}[c] (eV)	τ_{Ems} (ns)	ϕ	k_{ET}[d] (10^8 s^{-1})	k_{EnT}[e] (10^8 s^{-1})	k_{ET}[f] (10^8 s^{-1})	k_{BET}[g] (10^8 s^{-1})
$[Ru(ttpy)_2]^{2+}$	626	1.98		0.74	*h*				
1	626	1.98	1.82	0.76	*h*	*i*	*i*	*i*	*i*
2	620	2.00	1.85	0.58	*h*	*i*	*i*	*i*	*i*
3	626	1.98	1.83	0.87	*h*	*i*	*i*	*i*	*i*
4	620	2.00	1.85	0.64	*h*	*i*	*i*	*i*	*i*
$[Ru(bpy)_3]^{2+}$	584	2.12		890[5]	1[j]				
$[Ru(bpy)_2(4\text{-L-ph-bpy})]^{2+}$	588	2.11		1400[33]	∼1				
5	584	2.12	1.81	0.20	<0.001	50	*i*	*i*	70
6	594	2.08	1.84	6.4	∼0.01	1.2	0.31	0.26	>1.2
7	593	2.09	1.84	7.9	∼0.01	1.0	0.25	0.59	>1.0

[a] As PF_6^- salts. [b] Calculated from the emission at 77 K. [c] Calculated according to eq 1. [d] $Ru^*-NDI \rightarrow Ru^{III}-NDI^{\bullet-}$. [e] $Ru^*-NDI \rightarrow Ru-{}^3NDI$. [f] $Ru^*-NDI \rightarrow Ru^{III}-NDI^{\bullet-}$. [g] $Ru^{III}-NDI^{\bullet-} \rightarrow Ru-NDI$. [h] Quantum yield too low for quantification. [i] Not detected. [j] $\phi = 0.059$ for $[Ru(bpy)_3]^{2+}$ normalized to 1, 298 K.

correlated single photon counting experiments on the terpyridine complexes **1**−**4** showed only small differences in emission lifetime from the parent complex $[Ru(ttpy)_2]^{2+}$. In contrast, emission from the bipyridine complexes **5**−**7** was strongly quenched by the attachment of the NDI unit. The emission decay traces for **5**−**7** could be fitted to single-exponential functions with lifetimes of 0.20, 6.4, and 7.9 ns, respectively, as compared to ∼890 ns for $[Ru(bpy)_3]^{2+}$. Steady-state emission measurements of **6** and **7** gave an emission yield of 1% relative to $[Ru(bpy)_3]^{2+}$, while for **5** the yield was only 0.1%. This is in agreement with the shorter lifetime of the latter, as revealed by the time-resolved data.

Transient Absorption. Electron-transfer rates estimated from transient absorption and emission data are given in Table 3. The excited-state reactions of complexes **1**−**4** and **5** were studied by transient absorption pump−probe spectroscopy, following a 150-fs excitation pulse. For the terpyridine-type complexes **1**−**4**, only features from the excited state were observed. This decayed with a lifetime close to that of the parent complex $[Ru(ttpy)_2]^{2+}$ without producing any detectable charge-separated state.

In contrast, the charge-separated state of complex **5** was clearly seen in the transient absorption spectra (Figure 3). One hundred picoseconds after the excitation, a positive absorption originating from the $NDI^{\bullet-}$ radical is seen at 474 nm ($\epsilon \sim 23\,000$ M^{-1} cm^{-1}) and 605 nm ($\epsilon \sim 6400$ M^{-1} cm^{-1})[43] (Figure 3, dashed curve). The ratio of the difference absorption at 474 and 605 nm is not as high in Figure 3 as for the $NDI^{\bullet-}$ radical alone, because of the simultaneous bleach around 460 nm from the oxidized ruthenium(III) (solid curve). The transient absorption from the $Ru^{III}-NDI^{\bullet-}$ state decayed on the time scale of a few hundred picoseconds.

(41) Day, P.; Sanders, N. *J. Chem. Soc. (A)* **1967**, 1536−1541.
(42) Phifher, C. C.; McMillin, D. R. *Inorg. Chem.* **1986**, *25*, 1329−1333.
(43) Gosztola, D.; Niemczyk, M. P.; Svec, W. A.; Lucas, A. S.; Wasielewski, M. R. *J. Phys. Chem. A* **2000**, *104*, 6545−6551.

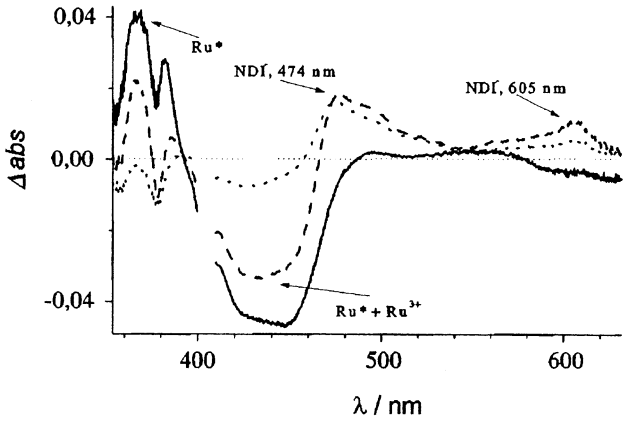

Figure 3. Transient absorption spectra of **5** probed at 10 ps (solid line), 100 ps (dashed line), and 400 ps (dotted line) after excitation (CH_3CN, $\lambda_{ex} = 400$ nm).

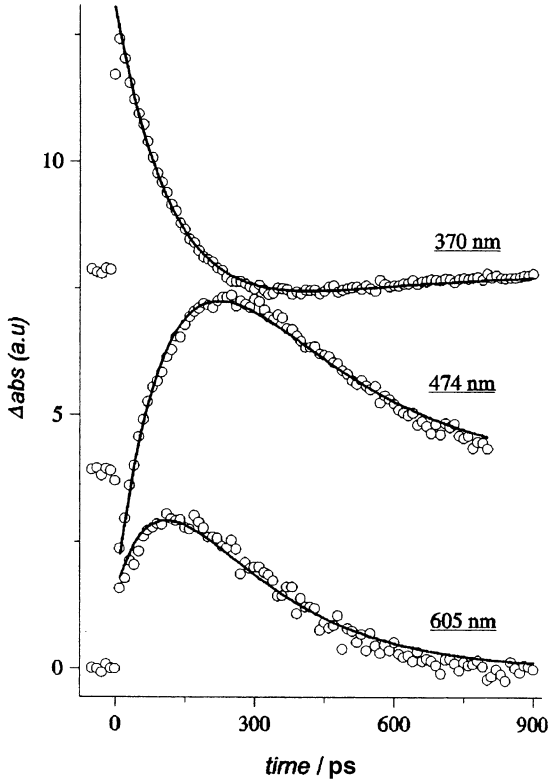

Figure 4. Transient absorption traces for **5** probed at 370 nm (top), 474 nm (middle), and 605 nm (bottom). The traces at 370 and 474 nm were vertically displaced for clarity (CH_3CN, $\lambda_{ex} = 400$ nm).

The dip centered at 378 nm in the spectrum, present already after 10 ps, can possibly be attributed to a low white light intensity due to high absorption from the NDI ground state.

Kinetic traces for **5** at 370, 474, and 605 nm (Figure 4) were fitted with a consecutive mechanism (excited state → charge-separated state → ground state) to determine the rates for forward and backward electron transfer. For the fitting procedures, the lifetime of the forward electron transfer (τ_f) was fixed at the value obtained from the emission lifetime experiments ($\tau_f = 200$ ps). The best fits (as judged by the χ^2 values and the residual plots) together with the data are shown in Figure 4. The lifetime for the electron back-transfer determined at the different wavelengths was $\tau_b = 140 \pm 30$ ps.

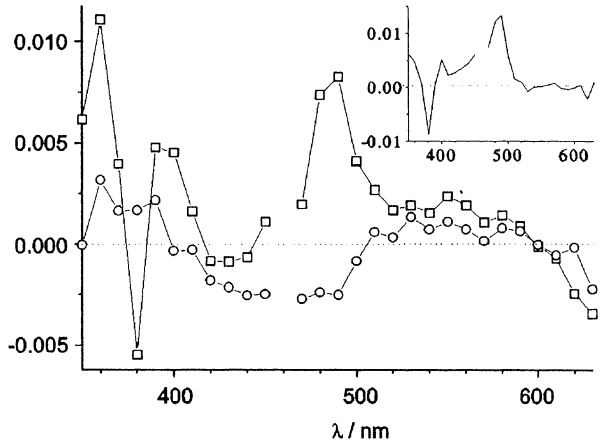

Figure 5. Transient absorption spectra of **6** recorded after 50 ns (squares) and 300 ns (circles) (CH_3CN, $\lambda_{ex} = 460$ nm). The result of subtraction of the 300 ns spectrum from that at 50 ns.

The rapid forward reaction for **5** ($\tau_f = 200$ ps) and the long lifetime of the parent complex $[Ru(bpy)_3]^{2+}$ (890 ns) suggest near 100% charge separation. The charge-separation yield was also estimated from the magnitudes of the initial excited-state bleach at 460 nm ($\Delta\epsilon = 10\,000$ M^{-1} cm^{-1})[44] and the maximum $NDI^{\bullet-}$ absorption at 605 nm ($\epsilon = 6400$ M^{-1} cm^{-1}). The maximum $NDI^{\bullet-}$ concentration reached 40% of the initial ruthenium(II) excited-state concentration. This is in very good agreement with what is expected from the kinetic data with a $\tau_f = 200$ ps forward reaction followed by a $\tau_b = 140$ ps recombination. Thus, the excited state is converted to the charge-separated state with a near 100% efficiency.

The quenching of complexes **6** and **7** was too slow to be followed on the pump−probe time scale. Instead, a nanosecond flash photolysis setup was used to follow the kinetics on a longer time scale. Figure 5 shows the transient absorption spectrum for **6** recorded 50 ns after excitation, after the excited-state had decayed (squares), and 300 ns after excitation (circles). The 300-ns spectrum is attributed to a small fraction (∼1%) of a long-lived $[Ru(bpy)_3]^{2+}$-like impurity. The inset in Figure 5 shows the spectrum after 50 ns with the contribution from the impurity subtracted. Comparison with literature data shows that this spectrum is dominated by the naphthalenediimide triplet (^{3}NDI),[45,46] although the transient spectrum of the $NDI^{\bullet-}$ radical is quite similar. The maximum around 485 nm in the ^{3}NDI spectrum is shifted to 474 nm in the $NDI^{\bullet-}$ spectrum; however, there is a pronounced absorption for $NDI^{\bullet-}$ all the way up to 605 nm, where $\epsilon = 6400$ M^{-1} cm^{-1}. For ^{3}NDI instead, the absorption is very small at $\lambda > 520$ nm. If our data would represent the radical, there should have been an absorption around 605 nm.

The decay kinetics for the ^{3}NDI state was probed at 490 nm, where the reference complex $Ru(bpy)_2$(4-L-tolyl-2,2′-bpy) (L is dipicolylamine) shows an isosbestic point between the ground and excited state.[47] A single-exponential fit to

(44) Yoshimura, A.; Hoffman, M. Z.; Sun, H. J. *Photochem. Photobiol. A: Chem.* **1993**, *70*, 29−33.
(45) Green, S.; Fox, M. A. *J. Phys. Chem.* **1995**, *99*, 14752−14757.
(46) Rogers, J. E.; Kelly, L. A. *J. Am. Chem. Soc.* **1999**, *121*, 3854−3861.

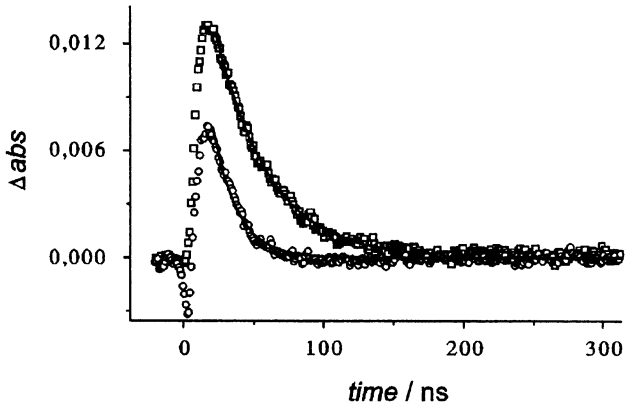

Figure 6. Transient absorption traces probed at 490 nm for **6** (squares), $\tau = 38$ ns, and **7** (circles), $\tau = 17$ ns (CH_3CN, $\lambda_{ex} = 460$ nm).

the decay of the kinetic traces at 490 nm gave $\tau = 38$ ns ($k = 2.6 \times 10^7$ s^{-1}) for **6** and $\tau = 17$ ns ($k = 5.9 \times 10^7$ s^{-1}) for **7** (Figure 6). The yield of ^{3}NDI estimated from the transient absorption at 490 nm ($\Delta\epsilon = 8000$ M^{-1} cm^{-1})[46] was ca. 20%. The initial excited-state yield for this comparison was measured with an isoabsorptive solution of the model $Ru(bpy)_2$(4-L-tolyl-2,2′-bpy) ($\Delta\epsilon_{460\ nm} = 10\,000$ M^{-1} cm^{-1}).[47] Because the excited ruthenium is ∼100% quenched, this shows that ∼80% of the excited ruthenium must have reacted via another pathway.

Discussion

The excited state of $[Ru(tpy)_2]^{2+}$ has a short lifetime ($\tau \sim$ 250 ps) and a low fluorescence quantum yield ($\Phi \sim 10^{-5}$).[42,48] This is mainly due to fast nonradiative decay through low-lying metal-centered dd-states. By substituting tolyl groups in the para-positions of the terpyridine units, it is possible to increase the excited-state lifetime to ∼1 ns. This is still a relatively short time if the goal is to perform redox chemistry from the excited state. Thus, for $[Ru(ttpy)_2]^{2+}$ to be used as an efficient photosensitizer, very fast electron donors or acceptors are required. Since naphthalenediimide has earlier been shown to induce subnanosecond oxidative quenching when linked to $[Ru(bpy)_3]^{2+}$-type photosensitizers,[26,27] it seemed possible to have efficient electron transfer also in the terpyridine-based complexes **1**−**4**. Unfortunately, as the results show, the attachment of the NDI acceptor gave at most a marginal difference from the data for the unsubstituted $[Ru(ttpy)_2]^{2+}$ (Table 3).[49] This indicates that the intrinsic decay of the excited state of the chromophore dominates over the desired electron transfer to the NDI unit, and based on the transient absorption spectra, we estimate that the concentration of charge-separated states could not be higher than 5% of the initial excited-state concentration at any time after the laser pulse.

In the corresponding bpy complexes **5**−**7**, an increased charge-separation yield would be expected because of the longer lifetime of the $[Ru(bpy)_3]^{2+}$ excited state ($\tau \sim$ 890 ns for the parent $[Ru(bpy)_3]^{2+}$ complex and ca. 1400 ns for the aryl substituted one) as compared to that for $[Ru(ttpy)_2]^{2+}$. There are two possible quenching mechanisms, either energy transfer to give the NDI triplet or through electron transfer to give the NDI radical. The driving force for energy transfer is modest, $-\Delta G°(EnT) = 0.05-0.09$ eV, as calculated from the difference between the E_{00} for the Ru ^{3}MLCT state and the ^{3}NDI state. The energy for the lowest lying ruthenium excited state, $E_{00}(^3MLCT)$, was calculated from the emission maximum at 77 K (Table 3). This is very close to the more rigorous value one would obtain from a spectral fit, as shown before for similar complexes.[50−52] $E_{00}(^3NDI) = 2.03$ eV, was obtained from literature data.[46] The driving force for electron transfer can be calculated from eq 1[53]

$$\Delta G^0(ET) = E_{1/2}(Ru^{3+/2+}) - E_{1/2}(NDI^{0/-}) - E_{00}(^3MLCT) + w(r) \quad (1)$$

where $E_{1/2}$, the electrochemical half-wave reduction potentials, are given in Table 1. The work term, $w(r)$, arising from Coulombic interactions between charges, is rather small in the present case, and in particular, the variation in $w(r)$ for our complexes is small and this contribution was therefore neglected. From the calculated values, $-\Delta G°(ET) = 0.24-0.31$ eV, it is clear that the driving force for electron transfer is considerably greater than for energy transfer.

The transient data for complex **5** (Figures 3 and 4) clearly show a ∼100% conversion of the initial ruthenium excited state to the charge-separated state with $\tau_f = 200$ ps followed by a recombination with $\tau_b = 140$ ps. The latter is longer than for related complexes with a viologen-type acceptor, ca. 30 ps,[11,13] but slightly shorter than with quinone as acceptor (1 ns).[24]

In complexes **6** and **7**, with a longer link between the ruthenium(II) and NDI units, slower electron transfer and a longer charge separation lifetime may be expected compared to the case for **5**. The forward reactions were indeed slower by more than an order of magnitude (Table 3) with $\tau_{em} =$ 6.4 and 7.9 ns for **6** and **7** respectively. No charge-separated state was seen in the spectra, however, suggesting that the back reaction is significantly faster than the forward reaction. Presumably, though, it is slower than the $\tau_b = 140$ ps for **5**, which has a much shorter intercomponent distance. The transient spectra for **6** and **7** instead show the features of the ^{3}NDI state, formed by energy transfer from the ruthenium(II) excited state with a ∼20% yield. The driving force for the energy transfer $-\Delta G°(EnT) = 0.05$ eV, while the driving force for electron transfer is more favorable with $-\Delta G°(ET) = 0.24$ eV. Thus, we conclude that the excited

(47) Abrahamsson, M. L. A.; Berglund-Baudin, H.; Tran, A.; Philouze, C.; Berg, K. E.; Raymond-Johansson, M. K.; Sun, L.; Åkermark, B.; Hammarström, L. *Inorg. Chem.* **2002**, *41*, 1534−1544.
(48) Stone, M. L.; Crosby, G. A. *Chem. Phys. Lett.* **1981**, *79*, 169.
(49) Because of perturbations by the linked NDI units, and the fact that **2** and **4** are mixed ligand tpy−ttpy complexes, the intrinsic lifetime in **1**−**4** cannot be expected to exactly equal the lifetime of the $[Ru(ttpy)_2]^{2+}$ model. Therefore, the small lifetime differences observed cannot be taken as evidence for electron transfer.
(50) Caspar, J. V.; Meyer, T. J. *Inorg. Chem.* **1983**, *22*, 2444−2453.
(51) Hammarström, L.; Barigelletti, F.; Flamigni, L.; Indelli, M. T.; Armaroli, N.; Calogero, G.; Guardigli, M.; Sour, A.; Collin, J.-P.; Sauvage, J.-P. *J. Phys. Chem. A* **1997**, *101*, 9061−9069.
(52) Treadway, J. A.; Loeb, B.; Lopez, R.; Anderson, P. A.; Keene, F. R.; Meyer, T. J. *Inorg. Chem.* **1996**, *35*, 2242−2246.
(53) Rehm, D.; Weller, A. *Isr. J. Chem.* **1970**, *8*, 259−271.

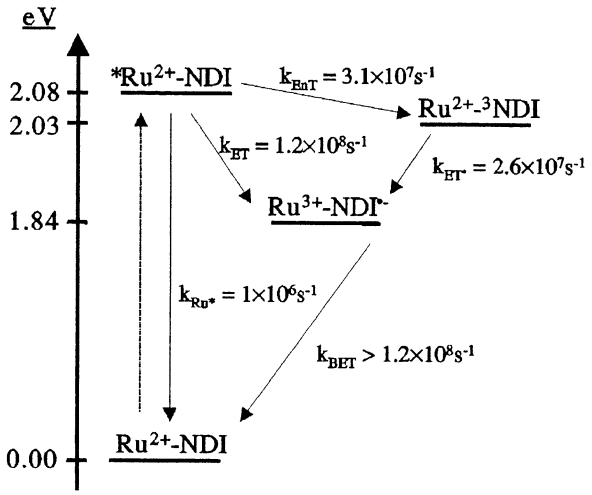

Figure 7. Photoreaction scheme for **6**.

ruthenium(II) ^{3}MLCT state is deactivated by a combination of these mechanisms, giving the rate constant as

$$1/\tau_{em} = 1/\tau_{Ru^*} + k_{ET} + k_{EnT} \quad (2)$$

with $\tau_{Ru^*} = 1400$ ns and $\tau_{em} = 6.4$ and 7.9 ns, respectively. With $k_{ET} = 4k_{EnT}$ (from the 80%/20% yield) we obtained the values for k_{ET} and k_{EnT} given in Table 3.

The ^{3}NDI state is normally long-lived ($\tau = 62$ μs).[46] We instead observed triplet lifetimes of 38 and 17 ns for 6 and 7. The only conceivable quenching mechanism for $Ru^{II}-{}^3$NDI is electron transfer from the ruthenium(II) moiety, giving the same $Ru^{III}-NDI^{\bullet-}$ state as for electron transfer from the ruthenium(II) ^{3}MLCT state. Since the $Ru^{III}-NDI^{\bullet-}$ state has a much shorter lifetime than the ^{3}MLCT and ^{3}NDI states, we only observe the rise and decay of the $Ru^{II}-{}^3$NDI state. The reaction scheme for **6** is given in Figure 7. Thus, it seems that charge separation is ~100% efficient in both **6** and **7**, and that 80% of the reaction occurs by direct electron transfer from the ruthenium(II) ^{3}MLCT state, while 20% occurs via formation of ^{3}NDI.

In contrast to these cases, the initial electron-transfer reaction in complex **5** is fast enough to totally out-compete the slower energy transfer to the $Ru^{II}-{}^3$NDI state.

When comparing the data for **6** and **7** it is interesting to note that the rate for the $*Ru^{II}-NDI \rightarrow Ru^{III}-NDI^{\bullet-}$ reaction is almost the same for the two complexes, despite the extra methylene link in **7**. Usually, the rate is reduced by a factor of ca. 4−5 with an additional methylene group.[54] For the second electron-transfer, $Ru^{II}-{}^3NDI \rightarrow Ru^{III}-NDI^{\bullet-}$, this effect is even more pronounced. This effect cannot be explained by the small (~10 meV) difference in $\Delta G°$ for **6** and **7** due to difference in $w(r)$. We believe instead that our observations can be explained by a difference in steric effects on the rotational angle between the planes of the phenyl and NDI groups. In **6**, the phenyl group and the NDI unit are directly attached to each other, and due to steric effects, they are forced to lie out of plane. In **7**, the additional methylene group leaves room for a more coplanar arrangement of the phenyl and NDI group, which should result in better electronic coupling. Thus, the decrease in coupling with distance would be compensated by a more coplanar arrangement in **7**.

The slower electron-transfer reactions in **6** and **7** as compared to **5** can be fully attributed to the ca. 5 Å longer transfer distance in the former complexes.

Conclusion

Two series of conformationally rigid donor−acceptor complexes based on ruthenium(II) tris(bipyridine) and bis(terpyridine) complexes linked to naphthalenediimide have been synthesized. The terpyridine complexes **1**−**4** showed no significant electron-transfer quenching. In contrast, efficient oxidative quenching was observed for the bipyridine complexes **5**−**7**. For complex **5**, the electron-transfer had a rate constant $k_{ET} = 5.0 \times 10^9$ s^{-1} for the forward reaction and $k_{BET} = 7.0 \times 10^9$ s^{-1} for the back reaction. It has been claimed earlier that energy transfer from a $Ru(bpy)_3^{2+}$-type sensitizer to NDI is improbable.[26] However, for the complexes **6** and **7**, which contain a phenyl link between the ruthenium and the NDI, our results suggest a biphasic forward electron transfer, in which 20% of the charge-separated state is formed via population of the ^{3}NDI excited state. The ^{3}NDI state has a lifetime of 38 ns for **6** and 17 ns for **7**, suggesting that it is quenched by electron transfer from ruthenium(II) to form the charge-separated state. Because the recombination reaction was faster than the forward electron transfer, the charge-separated state could not be observed directly. By comparing with the results for **5**, we estimate that the lifetime of the charge-separated state should lie between 200 ps and 5 ns. Although the systems **6** and **7** are not optimal from a steric point of view, these complexes seem promising for further functionalization.

Acknowledgment. We thank Prof. M. Wasielewski for informative and stimulating discussions. This work was financially supported by grants from the Knut and Alice Wallenberg Foundation, the Swedish National Energy Administration, and the Swedish Research Council.

IC020420K

(54) Bixon, M.; Jortner, J. *Adv. Chem. Phys.* **1999**, *106*, 35−202.